Nonlinearity and dynamic phase transition of charge-density-wave lattice

Chao-hung Du[a)]
Department of Physics, Tamkang University, Tamsui 251, Taiwan, Republic of China

Chung-Yu Lo, Hsiu-Hau Lin,[b)] and Shih-Lin Chang[c)]
Department of Physics, National Tsing-Hau University, Hsinchu 300, Taiwan, Republic of China

(Received 1 February 2007; accepted 3 April 2007; published online 31 May 2007)

We report the investigation of the dynamic behavior of charge-density waves (CDWs) in a quasi-one-dimensional material $K_{0.3}MoO_3$ using x-ray scattering and multiple x-ray diffraction. Under the application of voltages, we demonstrate that the occurrence of nonlinear conductivity caused by CDW is through the internal deformation of the CDW lattice, i.e., a phase jump of 2π, as the applied voltage exceeds the threshold. By measuring the evolution of peak width of satellite reflections as a function of the field strength, we also report that the CDW lattice can be driven to move and undergo a dynamic phase transition, i.e., from the disordered pinning state to ordered moving solid state, and finally, to disordered moving liquid. © *2007 American Institute of Physics*. [DOI: 10.1063/1.2738408]

I. INTRODUCTION

Nonlinearity is commonly observed in a very broad range of natural phenomena, from classical/quantum mechanics to biology, such as the squeezed states in a Bose-Einstein condensation[1] and the conduction of DNA.[2] The character of such behavior is the changes of the symmetry or the length scale of the states in the system. In condensed materials, the nonlinear physical properties always go along with the formation of a periodically modulated lattice caused by the inhomogeneous distribution of charges or spins, namely, charge- or spin-density waves, for instance, the nonlinear conductivity observed in $K_{0.3}MoO_3$ and $2H$-$NbSe_2$, or charge/spin stripes[3,4] in high-T_C superconductors and $La_{2-x}Sr_xNiO_4$, or other strongly correlated electron systems.

In such a periodically modulated system, its dynamic behavior caused by the interaction between the lattice and imperfections existing in the crystal is ubiquitous and has been a long-standing problem because of the correlation to the unusual physical phenomena, for instance, the charge-density waves/spin-density waves to the nonlinear conductivity, the charge/spin stripes to the colossal magnetoresistance (CMR) and the high-T_C superconductivity,[3] and the vortex lattice to superconductivity.[5] As in the static state, i.e., without the application of driving forces, the imperfections in a medium result in a disordered ground state which prevents the system from forming a long-range order at low temperatures, therefore giving rise to unusual physical properties. In dynamic systems under a driving force, the disordered medium produces a more fascinating phase diagram.[6,7] Analogous to the vortex lattice, the inhomogeneous distribution of charge densities also forms a periodic lattice below the transition temperature, namely, charge-density waves (CDWs).

In a system involving the instability of charge densities, its ground state can be expressed as $\rho=\rho_0[1+\Sigma_i P_i \cos(2\pi Q_i r+\varphi_i)]$, where ρ_0 is the undistorted electron density, P_i the distorted amplitude, $\mathbf{Q}_i$ the wave vector of the modulation, and φ_i the phase.[8] The appearance of imperfections distorts the lattice, and the phases φ_i are pinned by the imperfections. It has been demonstrated that the phase φ_i governs the dynamic behavior of this modulated lattice and is therefore responsible for the occurrence of the unusual physical phenomena, such as the pinning and memory effects and sliding behavior.[9] Theoretical investigations[6,7] predicted that the pinning forces become irrelevant when the system enters the sliding phase. This, indeed, provides a natural explanation for the dynamical narrowing of the half-width above the threshold voltage. However, to understand how the CDW adjusts to the pinning forces at different driving voltages, a direct measurement for the spatial distortions of CDW is desirable. In this report, in addition to the usual transport and full width at half maximum (FWHM) measurements of the CDW satellite reflections, we establish the connection between the lattice distortions and the triplet phase in x-ray scattering and thus demonstrate how the spatial distortions of CDW can be measured directly. While the sliding transition is already well studied, the technique we developed here can be applied to general periodic media driven by external sources and provides a different perspective into many interesting strongly correlated systems.

Since the triplet phase δ_3 of the multiple-wave diffraction plays an essential role in our study, it is helpful to illustrate its physical meaning and connections to lattice distortions. The triplet phase δ_3 is defined as the phase of the structure-factor triplet $F_{G_2}F_{G_3}/F_{G_1}$, where G_i are reciprocal lattice vectors and $G_1=G_2+G_3$.[10–12] Since they form a closed triangle in the reciprocal vector space, it is straightforward to show that the triplet phase δ_3 is invariant under arbitrary choices of unit cells.[13] This invariance provides a hint for its connection to some physical quantity, which turns out to be the internal distortion of the unit cell. Experimentally, this

a)Electronic mail: chd@mail.tku.edu.tw
b)Also at Physics Division, National Center for Theoretical Science, Hsinchu 300, Taiwan.
c)Also at National Synchrotron Radiation Research Center, Hsinchu 300, Taiwan.

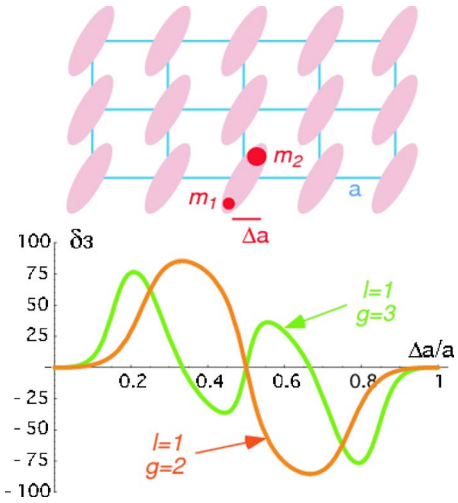

FIG. 1. (Color online) (a) (Top) Two-dimensional square lattice with distortion Δa. (b) (Bottom) Triplet phase δ_3 vs the distortion $\Delta a/a$. Two specific choices $l=1$, $g=2$ and $l=1$, $g=3$ are presented here.

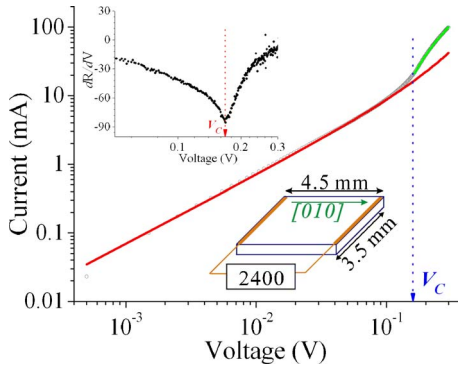

FIG. 2. (Color online) *I-V* characteristic of $K_{0.3}MoO_3$ in a two-probe transport setup at $T=70$ K. The data are displayed as the log-log plot. The red line shows the linear behavior due to the thermal creeps of CDWs below the transition point V_C, and the green line is the best fit of the data, for $V > V_C$, to a power law $I \propto [(V-V_C)/V]^{\beta}$. The inset for (dR/dV) clearly shows a dip at the V_C.

triplet phase can be determined by measuring the diffracted intensity profiles of a three-wave $(\boldsymbol{O},\boldsymbol{G_1},\boldsymbol{G_2})$ diffraction involving the $\boldsymbol{G_1}$ primary reflection, $\boldsymbol{G_2}$ secondary reflection, and coupling $\boldsymbol{G_3}=\boldsymbol{G_1}-\boldsymbol{G_2}$ reflection. $\boldsymbol{O}$ stands for the direct reflection of the incident beam.[10] Let us consider a two-dimensional square lattice with two ions in one unit cell, as shown in Fig. 1. Without distortion, $\delta a=0$, the lattice has inversion symmetry which ensures all structure factors are real (under appropriate choice of the unit cell) and thus gives $\delta_3=0$. Under the driven voltage, the CDW is distorted and twists the underlying lattice as well. For simplicity, let us assume that it can be described by a lattice twist δa along the direction of the CDW (x axis here). Furthermore, let us choose the reciprocal lattice vectors to be along the direction of the CDW, i.e., $\boldsymbol{G_1}=-(2g\pi/a,0)$, $\boldsymbol{G_2}=(2l\pi/a,0)$, and $\boldsymbol{G_3}=\boldsymbol{G_1}-\boldsymbol{G_2}$. The resultant triplet phase can be computed straightforwardly,

$$\tan\delta_3 = \frac{\Delta\sum_i \sin(G_i\delta a+\varphi_i)}{r+\sum_i \cos(G_i\delta a)},$$

where $\varphi_1=\pi$ and $\varphi_{2,3}=0$. The other parameters are $\Delta=(m_1-m_2)/(m_1+m_2)$ and $r=(m_1^3+m_2^3)/2m_1m_2(m_1+m_2)$. Two particular choices of l and g are given in Fig. 1 to demonstrate the connection between the triplet phase δ_3 and the lattice distortion δa.

In the realistic setup, the lattice distortion is rather small $\delta a/a \ll 1$ at all applied voltages, thus the expression of the triplet phase simplifies, $\delta_3 \sim (\delta a/a)^3$. Note that the cubic dependence is generic due to the inversion symmetry of the undistorted lattice and the zero vector sum of $\boldsymbol{G_i}$. While this result is derived from the simple model, it captures the generic dependence of the triplet phase even for the more complicated crystal $K_{0.3}MoO_3$ we studied here. Therefore, the triplet phase provides a direct measurement of the spatial distortion of CDW at different driving voltages.

II. EXPERIMENT AND DISCUSSION

Now we turn to the experimental details and the observed results of transport and x-ray measurements. A good quality single crystal $K_{0.3}MoO_3$, being a quasi-one-dimensional material, was used for this study. The crystal structure belongs to the monoclinic system with a space group $C2/m$. The lattice parameters of $K_{0.3}MoO_3$ are $a=18.162$ Å, $b=7.554$ Å, $c=9.816$ Å, and $\beta=117.393°$.[14] The sample was characterized to have a mosaic width of ~0.005° and prealigned using an x-ray rotating anode source. The *in situ* measurements were carried out on the beamline BL12B2 of SPring-8 synchrotron facility. Two gold stripes spaced ~3 mm were evaporated onto the sample surface as shown in the inset of Fig. 1, so that the voltage was applied along the b^*, [010], axis. The sample was glued on the cold head of a cryostat mounted on a six-circle diffractometer. A Keithely 2400 source meter was used to generate the driving voltage, and the *I-V* curve was measured in the two-probe setup. An upper limit of the current was set to 300 mA in order to protect the sample and meter.

Figure 2 shows the nonlinear conductivity of the sample at $T=70$ K, indicating the transition from pinned CDWs to sliding CDWs. Best fits to the data for the low voltage region, the *I-V* curve can be fitted well by an exponential formula as reported by Ogawa *et al.*,[15] indicating a CDW creeping behavior. However, we did not observe the switching phenomenon[16] at V_C for $T=70$ K because of thermal fluctuations smearing out the switching transition.[17] For the higher voltage regime, the data were fitted to a power law, $I \propto [(V-V_C)/V_C]^{\beta}$, giving rise to the threshold $V_C=0.165$ V and an exponent $\beta=1.114$, suggesting that the sliding CDWs behave in a dynamic critical behavior.[18–21] This is also analogous to the motion of a disordered flux lattice observed in $2H$-$NbSe_2$, in which the scaling between the driving force and velocity gives rise to a high exponent.[22] This suggests that the coupling between the imperfections and dimensionality could play an important role as the driving force exceeds the threshold. The threshold voltage V_C for sliding CDWs was also confirmed by a plot of dR/dV vs V (the inset of Fig. 2).

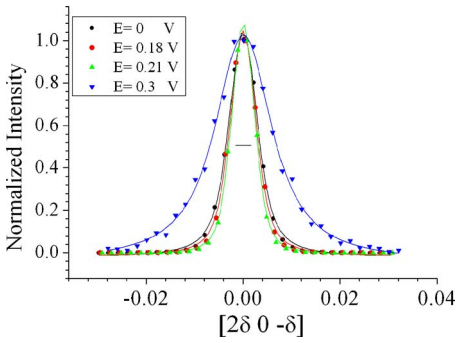

FIG. 3. (Color online) Evolution of the peak profile of CDW satellite reflection at different voltages along the longitudinal direction [2 0 −1]. The solid lines are the best fits convoluted with the resolution function. The bar shows the resolution as obtained from a nearby Bragg reflection (12 0 −6).

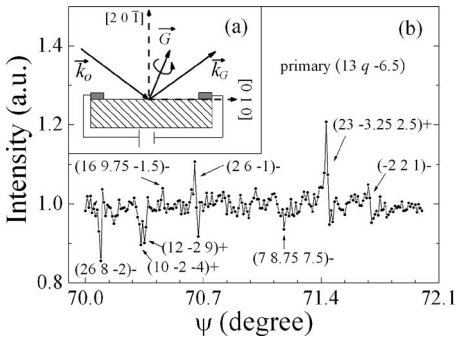

FIG. 4. Azimuthal scan of three-wave diffraction around the primary reflection ***G***. Major peaks and dips are indexed in accordance with the calculation of multiple diffraction pattern. The inset shows the experimental setup schematically. The seemingly noisy background is caused by the presence of many weak fractional reflections.

Firstly, we report the evolution of CDW satellite reflection as a function of voltage, which was probed *in situ* using x-ray scattering. Since the formation of density modulations occurs at $T_c \approx 180$ K, the sample was cooled down to 70 K. The satellite reflection was located at the Bragg position $G=(13\ q\ 6.5)$, where $q \sim 0.748$. Scans were performed through the longitudinal direction of, [2 0 −1], and the data were convoluted with the x-ray resolution function obtained from the nearby Bragg peak (12 0 −6). As shown in Fig. 3, we observed the narrowing of the CDW satellite reflection for $0.165\ \text{V} < V < 0.22$ V, and then broadening for $V > 0.23$ V. As summarized in Fig. 7(a) below, $V_C \sim 0.165$ V, where the creeping CDWs occur, the FWHM remain unchanged. This means that the ordering of the quenched disordered CDWs was not altered by the low driving force in this region. Beyond the threshold V_C, the CDW reflection gets sharper but weaker. This can be understood by the fact that a driving force steers a pinned lattice and results in inhomogeneous flow.[23,24] As the driving force exceeds the threshold, $V_C \sim 0.165$ V, the CDW lattice reorders along the longitudinal direction [2 0 −1], transverse to the field direction. As the CDWs are driven to sliding along the direction [0 1 0], the coupling between the chains is further reduced,[25] and could result in the transition toward the smectic type of order[6,27] in region II. In this region, because of lack of switching behavior at the threshold V_C, the motion of CDW lattice can be described as the critical phenomenon of a classical field associated with distortions and is still in an elastic flow state.[16,20] As the voltage exceeds 0.18 V, the lattice shows a long-range-ordered state: temporal order. This motional ordered behavior by a driving force has also been reported in the $NbSe_3$.[26] In contrast to the lattice existing near the threshold (V_C=0.165 V), where both pinned and flowing regions coexist, there only the flowing part remains in this motional ordered state; namely, a moving solid phase.[21,25,26] When $V > 0.22$ V, we observed continuous broadening of the width and decreasing amplitude of the diffraction peak as the critical scattering, indicating that the moving solid phase starts deforming and then becomes a moving electronic liquid phase.

The other key quantity we studied is the triplet phase δ_3 of a three-wave multiple diffraction at different biased voltages. To set up a three-wave $(\boldsymbol{O},\boldsymbol{G},\boldsymbol{L})$ multiple diffraction experiment, the crystal is first aligned for a reflection G, the so-called primary reflection. It is then rotated around the reciprocal lattice vector $\boldsymbol{G}$ with an azimuthal angle ψ to bring in the secondary reflection $\boldsymbol{L}$, which also satisfies Bragg's law. Namely, both $\boldsymbol{G}$ and $\boldsymbol{L}$ reflections take place simultaneously. $\boldsymbol{O}$ stands for the incident reflection. The interaction of the multiply diffracted waves modifies the intensity of the primary reflection. A portion of the multiple diffraction pattern of the primary reflection G is shown in Fig. 4. Note that the azimuthal angle was measured counterclockwise from [0 1 0] direction. The horizontal background is due to the reflection $\boldsymbol{G}$. Relative intensity peaks and dips are marked with Miller indices of the secondary reflection $\boldsymbol{L}$. Thereafter, a multiple-wave diffraction is denoted as $L/(G-L)$ and the in and out positions are indicated by "+" and "−" signs, respectively. Intensity variation showing asymmetric distribution versus ψ gives the information about δ_3, which is the phase of the structure-factor triplet $F_L F_{G-L}/F_G$, where F_G, F_L, and F_{G-L} are the structure factors of the primary reflection **G**, the secondary reflection **L**, and the coupling reflection **G−L** involved in the three-wave diffraction.[10–12] Previously,[28,29] we demonstrated that the triplet phase δ_3 due to the coupling between the CDW lattice and its host lattice can be probed using multiple diffraction. Here we further demonstrate that measuring the relative change in $\delta_3, \Delta\delta_3$, caused by a driving force, makes the study of the internal deformation of the CDW lattice possible.

We concentrated on the particular three-wave diffraction, (0 0 0), (13 q −6.5), and (4 −8 4), at ψ=108.53°, where the primary reflection is (13 q −6.5) and the coupling reflection is (9 8+q 10.5). The profile asymmetry of the diffraction intensity of (13 q −6.5) versus ψ at V=0 is typical for δ_3 =0. The phase variation $\Delta\delta_3$ due to nonzero applied voltages was analyzed based on the dynamical theory for multiple diffractions.[10,12] Figure 5 displays the evolution of the profile as a function of applied voltage. Clearly, the profile develops different asymmetries only as the voltage approaches V_C, and then returns to the original value at low voltages. In the static CDW state, the crystal lattice possesses a centrosymmetric structure, and a change in the peak profile means that this centrosymmetry is broken due to the relative motion of ions

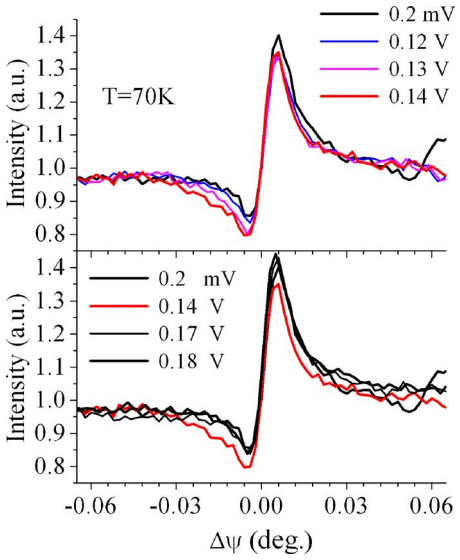

FIG. 5. (Color online) Evolution of the peak profile from the three-wave diffraction pattern as a function of applied voltage. Changes in the profiles can be seen clearly only as the applied voltages approach V_C=0.16 V.

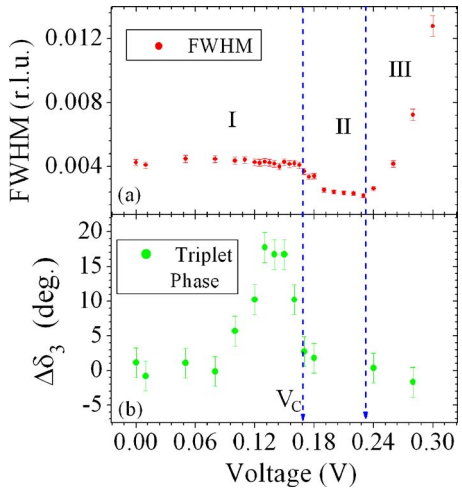

FIG. 7. (Color online) (a) Evolution of FWHM of the CDW satellite reflection as a function of applied voltage. According to the changes of the peak width, the CDWs can be classified into three phases: (I) the creeping CDW state, (II) the moving solid, and (III) the moving liquid. (b) The triplet phase change $\Delta\delta_3$ at different voltages. Note that in the sliding phase, $\Delta\delta_3$=0 is the direct evidence that the pinning forces become irrelevant.

by a driving force. This results in a nonzero $\Delta\delta_3$. The rocking curve width of a Bragg reflection was also monitored in order to make sure that the crystal was not destroyed by applied voltages. Figure 6 shows two cases of the best fits of the triplet phase $\Delta\delta_3$ at V=0.2 mV and 0.14 V. The analysis is based on the dynamic theory for multiple diffraction.

As shown in Fig. 7(b), the $\Delta\delta_3$ reaches maximum at V =0.12–0.14 V. This can be understood as the internal distortion of CDWs is saturated just before the sliding motion. Classically, upon the application of bias voltage, the free energy is minimized by the elastic energy cost due to CDW distortion. After threshold, it is energetically favorable to slid (increasing kinetic energy) rather than hold up the large elastic energy. The estimated $\Delta\delta_3$ from curve fitting at 0.1, 0.12, 0.13, 0.14, 0.15, and 0.16 V are about 6°, 10°, 18°, 17°, 17°, and 10°, respectively, and then decreases to 0° for V >0.18 V, as shown in Figs. 5 and 7(b). This evidences experimentally that the occurrence of nonlinear transport behavior is through a phase jump of 2π at the sliding threshold, i.e., from the pinned to sliding states.

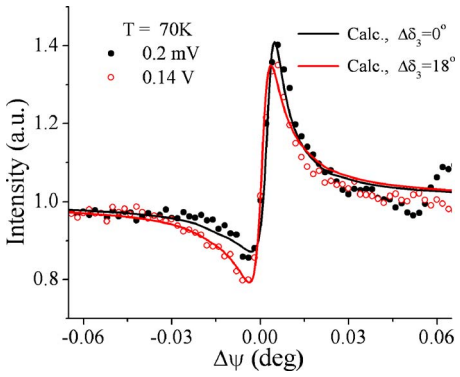

FIG. 6. (Color online) Triplet phase change $\Delta\delta_3$ extrapolated from curve fitting of the three-wave diffraction profiles. The analysis is based on the dynamic theory for multiple diffraction, giving $\Delta\delta_3$=0° and 18° at V =0.2 mV and 0.14 V, respectively.

CONCLUSION

Based on all experimental results given above, the simultaneous studies on I-V curve, the relative phase change $\Delta\delta_3$, and the ordering the CDWs as a function of driving voltage have provided evidence for the origin of the nonlinearity and the dynamic phase transition of a periodic medium. The phase measurement using three-beam diffraction is also demonstrated as a sensitive way to study the transport phenomena in nonlinear systems. While it is already exciting to observe these dynamic motions of CDW, it also opens up many interesting issues requiring further studies. For instance, crossovers between different types of dynamics could be achieved by varying temperature, a global phase diagram can be mapped out completely by varying temperature and driving force, and a deeper understanding of the dynamic motions of a periodic medium such as that existing in the high-T_C related perovskites can be achieved.

ACKNOWLEDGMENTS

The authors acknowledge the National Science Council in Taiwan for financial support, through Grant No. NSC 94-2112-M-032-004, and the National Synchrotron Radiation Research Center for allocation of beam time and technical support during the experiment.

[1]C. L. Rolston and W. D. Phillips, Nature (London) **416**, 219 (2002).
[2]D. Porath, A. Bezryadin, S. de Vries, and C. Dekker, Nature (London) **403**, 635 (2000).
[3]P. Littlewood, Nature (London) **399**, 529 (1995).
[4]C.-H. Du *et al.*, Phys. Rev. Lett. **84**, 3911 (2000).
[5]U. Yaron, Nature (London) **376**, 753 (1995).
[6]T. Giamarchi and P. De Doussal, Phys. Rev. B **52**, 1242 (1995).
[7]L. Balents, M. C. Marchetti, and L. Radzihovsky, Phys. Rev. B **57**, 7705 (1998).
[8]A. W. Overhauser, Adv. Phys. **27**, 343 (1978).
[9]G. Grüner, *Density Waves in Solids* (Addison-Wesley, New York, 1994).
[10]S. L. Chang, *X-ray Multiple-wave Diffraction: Theory and Application* (Springer-Verlag, Berlin, 2004).
[11]R. Colella, Acta Crystallogr., Sect. A: Cryst. Phys., Diffr., Theor. Gen.

Crystallogr. **30**, 413 (1974).
[12]Q. Shen, Phys. Rev. Lett. **80**, 3268 (1998).
[13]C. Giacovazzo, *Fundamentals of Crystallography* (Oxford University Press, Oxford, 2002).
[14]W. J. Schutte and J. L. de Bore, Acta Crystallogr., Sect. B: Struct. Sci. **49**, 579 (1993).
[15]N. Ogawa, N. A. Shiraga, R. Kondo, S. Kagoshima, and K. Miyano, Phys. Rev. Lett. **87**, 256401 (2001).
[16]V. M. Vinokur and T. Nattermann, Phys. Rev. Lett. **79**, 3471 (1997).
[17]T. L. Adelman, T. L. Adelman, J. McCarten, M. P. Maher, D. A. DiCarlo, and R. E. Thorne, Phys. Rev. B **47**, 4033 (1993).
[18]P. Chauve, T. Giamarchi, and P. Le Doussal, Phys. Rev. B **62**, 6241 (2000).
[19]M. C. Marchetti, A. A. Middleton, K. Saunders, and J. M. Schwarz, Phys. Rev. Lett. **91**, 107002 (2003).
[20]D. S. Fisher, Phys. Rev. Lett. **50**, 1486 (1983).
[21]L.-W. Chen, L. Balents, M. P. A. Fisher, and M. C. Marchetti, Phys. Rev. B **54**, 12798 (1996).
[22]S. Bhattacharya and M. J. Higgins, Phys. Rev. Lett. **70**, 2617 (1993).
[23]A. E. Koshelev and V. M. Vinokur, Phys. Rev. Lett. **73**, 3580 (1994).
[24]C. Reichhardt, C. J. Olson, I. Martin, and A. R. Bishop, Phys. Rev. Lett. **90**, 026401 (2003).
[25]S. G. Lemay, R. E. Throne, Y. Li, and J. D. Brock, Phys. Rev. Lett. **83**, 2793 (1999).
[26]R. Danneau *et al.*, Phys. Rev. Lett. **89**, 106404 (2002).
[27]P. Le Doussal and T. Giamarchi, Phys. Rev. B **57**, 11356 (1998).
[28]C.-H. Du, M.-T. Tang, Y.-R. Lee, Y. P. Stetsko, C.-W. Wang, C.-W. Cheng, and S.-L. Chang, Acta Crystallogr., Sect. A: Found. Crystallogr. **60**, 209 (2004).
[29]C.-H. Du, M.-T. Tang, Y.-R. Lee, Y. P. Stetsko, C.-Y. Lo, J.-J. Lee, H.-H. Lin, and S.-L. Chang, Appl. Phys. Lett. **88**, 241916 (2006).